CONVERGENCE AND SUBDUCTION AT THE NORTH EQUATORIAL FRONT

A THESIS SUBMITTED TO THE GRADUATE DIVISION OF THE UNIVERSITY OF HAWAII IN PARTIAL FULFILLMENT OF THE REQUIREMENTS FOR THE DEGREE OF

MASTER OF SCIENCE

IN

OCEANOGRAPHY

DECEMBER 1996

By

Michael Sawyer

Thesis Committee:

Pierre Flament, Chairperson
Doug Luther
Gary Barnes

We certify that we have read this thesis and that, in our opinion, it is satisfactory in scope and quality as a thesis for the degree of Master of Science in Oceanography.

THESIS COMMITTEE

Chairperson

Acknowledgments

The work described in this thesis was conducted in the framework of the Tropical Instability Wave Experiment. Funding was provided by the National Science Foundation (grants OCE-8818732, REU-8900858, OCE-8922207 and OCE-9117078) and the National Aeronautics and Space Administration (grant SIRC-093). This project provided a rich collection of data previously unavailable in any form, without which this work could never have been completed.

I wish to thank Pierre Flament, Gary Mitchum, Doug Luther, and Gary Barnes for serving on my Master's Committee and for their patient help in preparing this manuscript. In addition, Eric Firing, Roger Lukas, and Rudolf Kloosterziel provided valuable input on various aspects of this work.

The Physical Oceanography Graduate Student (POGS) group and Na'kama'kai, the graduate association in the Dept. of Oceanography provided invaluable support and input while preparing the oral defense and manuscript. In particular, Sean Kennan, Jim Potemra, Rick Lumpkin, Sophia Ashgar, Kathy Donahue, and Julia Hummon assisted in reviewing early drafts of this manuscript and listening to countless rehearsals of my oral defense.

It would be impossible to list everyone involved in the field research and initial data analysis of the Tropical Instability Wave Experiment, but their hard work was invaluable. Ken Shultis, Will Harvig, and Dave Gravatt of the University of Hawaii Shipboard Technical Operations Group and the crew of the *R/V Moana Wave* provided an excellent platform on which to collect these data. Acoustic Doppler Current Profiler data was collected with the support of Eric Firing's research group and analyzed by June

Firing. SeaSoar data was collected with the cooperation of the J. Luyten, W. Ostrum, and J. Thompson from the Woods Hole Oceanographic Institution and V. Lawford from Chelsea Instruments. The CTD system was maintained by Ken Constantine from the University of Hawaii. The Air-Sea Interactions package was designed by Pierre Flament, Uli Knirch, Ken Constantine, Bob Cunningham, Alton Goo, Hans Ramm, Mike Simpson, and Christian Trefois.

Finally, there are a number of people without which I would not even have become involved in oceanography to begin with. Charlie Johnson and Steven Reynolds at the North Carolina State University Dept. of Physics and John Morrison at the North Carolina State University Dept. of Marine and Atmospheric Sciences provided the early training and direction leading me to this work.

Presented in loving memory of Mack V. Sawyer II.

Abstract

Satellite thermal data from the equatorial Pacific show strong, seasonally dependent upwelling along the equator, characterized by a sharp front between the cold upwelling water and the warmer surrounding water to the north and south. Strong wave-like perturbations have been observed on this front, caused by meridional oscillations in response to the passage of Tropical Instability Waves, moving westward at 20 to 50 km/day with wavelength of 500 to 1000 km. This study, conducted in the framework of the Tropical Instability Wave Experiment, will focus on the small-scale dynamics of the front itself. Strong convergence is found in leading- and trailing-edge crossings of the front, resulting in subduction of the equatorial upwelling water below surrounding warmer waters, having potential significant impact on local biological processes. As the layer is subducted, a strong along-front jet is formed, moving to the east following the curvature of the front. Based on Temperature-Salinity properties of this jet, it serves to transport high-salinity water toward the north away from the equator, gradually mixing with surrounding water.

Table of Contents

List of Figures

List of Abbreviations

- ADCP Acoustic Doppler Current Profiler
- AVHRR Advanced Very High Resolution Radiometer
- CTD Conductivity, Temperature, and Depth profiler
- EqPac JGOFS Equatorial Pacific Leg
- EUC Equatorial Under-current
- GPS Global Positioning System
- ITCZ Inter-Tropical Convergence Zone
- JGOFS Joint Global Ocean Flux Study
- MCSST Multi-Channel Sea Surface Temperature
- MW9010 Moana Wave cruise 90-10
- MW9012 Moana Wave cruise 90-12
- NEC North Equatorial Current
- NECC North Equatorial Counter-current
- NOAA National Oceanic and Atmospheric Administration
- PMEL Pacific Marine Environmental Lab
- Ri Richardson Number

- SRL Shuttle Radar Laboratory
- SST Sea Surface Temperature
- TC9407 Townsend Cromwell cruise 94-07
- TIWE Tropical Instability Wave Experiment
- TS Temperature-Salinity
- SEC South Equatorial Current
- SRL Shuttle Radar Laboratory
- UTC Universal Time Code
- WOCE World Ocean Circulation Experiment

Chapter 1

Introduction

The objective of this thesis is to study the dynamics and thermohaline structure of the North Equatorial front, separating the Pacific equatorial upwelling water from the warmer tropical water to the north. High-speed sampling of temperature, salinity, velocity, and meteorological data was conducted in a number of frontal crossings, coupled with Lagrangian drifter studies, satellite thermography, and moorings in the vicinity of the front. Three specific regions will be discussed, as seen in Figure 1.1. The leading edge crossing refers to a crossing made on the western side of a perturbation in the North Equatorial Front, the trailing edge crossing was conducted on the eastern side of a perturbation, and the northern boxes were conducted at the northern extent of a perturbation.

1.1 Equatorial Current System Overview

Equatorial currents and water properties are strongly influenced by local atmospheric forcing. During the northern hemisphere winter, the Inter-Tropical Convergence Zone (ITCZ), located approximately between 5°N and 10°N is characterized by increased rainfall and reduced wind stress. The northeasterly trade winds lie to the north of the ITCZ and the southeasterly trades lie to the south.

The mean flow in this area consists of alternating regions of eastward and westward flowing currents, as seen in Figure 1.2 [Philander, 1990a]. The North Equatorial Current (NEC) and South Equatorial Current (SEC) are part of the anticyclonic current gyres of the north and south hemispheres, respectively. The NEC, located to the north of 10°N

has speeds generally less than 0.2 ms^{-1} westward. The SEC, located south of 3°N has a velocity reaching 1.0 ms^{-1} westward between the equator and 3°N, dropping to 0.1 ms^{-1} south of the equator. Between the NEC and SEC is the North Equatorial Counter-current (NECC), moving to the east with a velocity of around 0.5 ms^{-1}. The Equatorial Under-current (EUC) is a strong eastward-flowing jet with velocities reaching 1.50 ms^{-1} extending along the equator from around 50m depth to the permanent thermocline at around 150 dbar.

The Equatorial Pacific can be divided up into three distinct regions. From 90°W to 160°W is a region of strong upwelling driven by the divergence in the Ekman forcing as f changes sign along the equator. This upwelling region manifests itself as a tongue of cool water extending from the coast of South America toward the west, often reaching as far as the international date line [Cromwell, 1953; Cox, 1980]. Between 120°W and the date line, the upwelling becomes weaker, and the cold tongue becomes less prominent toward the west. West of the date line, the Western Pacific Warm Pool becomes the dominant feature of the region. This thesis will focus on the region between 90°W and 140°W.

Because equatorial surface currents are largely driven by wind stress curl from the trade-wind system, seasonal variation in the wind forcing will result in a similar variation in the strength of the equatorial currents. During periods of weakened southeast trades (Northern hemisphere spring), the equatorial surface currents are weakened. Reduced equatorial upwelling results from decreases in Ekman forcing. As the trade winds strengthen during Northern hemisphere fall, the surface currents increase and equatorial upwelling begins.

1.2 The North Equatorial Front

Sharp fronts are observed on the boundary between upwelling waters and warmer waters to the north and south. The North Equatorial Front is the boundary between the equatorial upwelling water and the warmer water to the north. Satellite Sea Surface Temperature (SST) images show temperature gradients of at least $1°\text{Ckm}^{-1}$, probably a low estimate limited by instrument resolution.

The amplitude of the front is largely a function of the magnitude of the upwelling. Figure 1.3 shows a series of satellite SST images collected May 7, May 26, and June 11, 1990. With the increase in northeast trades at the end of May, the upwelling is strengthened, increasing thermal gradients across the front. The strongest fronts are observed near the Peru coast, where the upwelling is greatest and the equatorial waters the coldest. Moving toward the west, upwelling is reduced, the cold tongue is weakened, and thermal gradients along the front are reduced. The dynamics west of the dateline are significantly different from those to the east, due to the influence of the warm pool on the surrounding waters.

1.3 Instabilities of the Equatorial Current System

Strong wave-like perturbations have been observed on the North Equatorial Front, caused by meridional oscillations in response to the passage of Tropical Instability Waves [Legeckis, 1977; Legeckis, 1986; Luther and Johnson, 1990; Johnson and Luther, 1994, and others]. These perturbations propagate westward at 20 to 50 km day^{-1} with meridional amplitudes reaching 500 km and zonal wavelengths of 500 to 1,000 km. Equatorial instabilities of this form were first observed in the Atlantic [Düing *et al.*, 1975], using

data from moored current meters. The first observation in the the Pacific was by Legeckis [1977] using satellite SST images. These perturbations contribute to the meridional eddy fluxes of momentum and heat playing a major role in the dynamical coupling of the currents in the equatorial current system.

Using a stability analysis of idealized equatorial currents, Philander [1978] suggests that the shear of the SEC or the shear between the SEC and NECC may be the primary source of instability. Hansen and Paul [1984] and Weisberger and Weingartner [1988] support this analysis using moored current meters and Lagrangian drifters. However, Cox [1980] and Hansen and Paul [1984] suggest that conversion of mean thermocline slope to eddy energy through baroclinic instability may play a role in generating tropical instability waves. Luther and Johnson [1990] find that barotropic instability between the SEC and EUC is most important during the boreal Summer, baroclinic conversions from 2-6°N during Winter, and baroclinic instabilities in the NECC thermocline most important during Spring.

1.4 Objectives of the Tropical Instability Wave Experiment

The Tropical Instability Wave Experiment (TIWE) was designed to test hypotheses of instability wave generation and interaction with zonal wave current systems in the Pacific and to understand the effects of the North Equatorial Front on the local oceanic and atmospheric environment. Previous field investigations have provided different views of the temporal and spatial structure of Instability waves; time series at a few fixed points, surface temperature, and synoptic velocity sections were often obtained as part of studies designed for different purposes. In contrast, TIWE was organized specifically to sample

the temporal and spatial progression of Equatorial Instability Waves over complete wave cycles.

Here we will focus on the structure of the equatorial front itself. Of special interest will be the northern crests of the perturbations, associated with poleward jets of cold haline water, which may play a significant role in meridional fluxes away from the equator. Mechanisms responsible for their growth and mixing properties will be discussed.

Convergence is required to maintain fronts in the ocean (or atmosphere). Thermohaline and velocity structures will be analyzed to quantify this convergence. Finally, connections to biological activity along the front will be explored.

The following points will be addressed:

- What is the thermohaline structure of the water column on either side of the front, and what dynamics are inferred from these thermohaline structures. In particular, can vorticity balances be applied.

- How strong is the surface convergence field along the front, and is it consistent in all regions.

- How is the biological activity in the region affected by these fronts? Do the fronts increase or decrease the productivity compared to that driven by the upwelling alone?

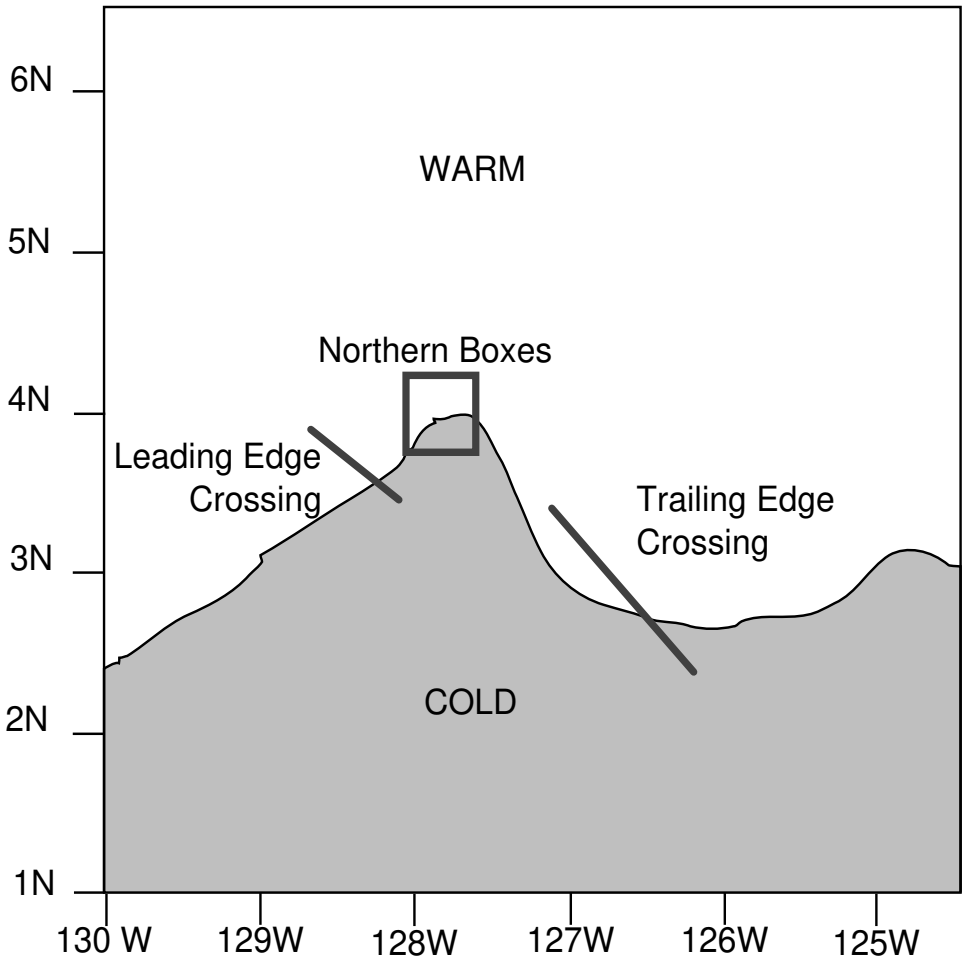

Figure 1.1: Schematic diagram of data used in this experiment. The gray area represents cold equatorial upwelling water and the white area represents warmer surrounding water. The location of the front is hand-traced from the satellite image on day 232, 01:59UTC, collected during the leading-edge crossing. The northern box and trailing-edge crossing have been translated at the phase speed of the perturbation. The leading-edge crossing was conducted in a line from the northwest to the southeast and the trailing-edge crossing was conducted from the southeast to the northwest. The northern boxes were conducted in alternating clockwise and counter-clockwise patterns.

Figure 1.2: A schematic diagram of the horizontal and vertical circulation in the tropical Pacific Ocean. *From Philander, et al. [1990b]*

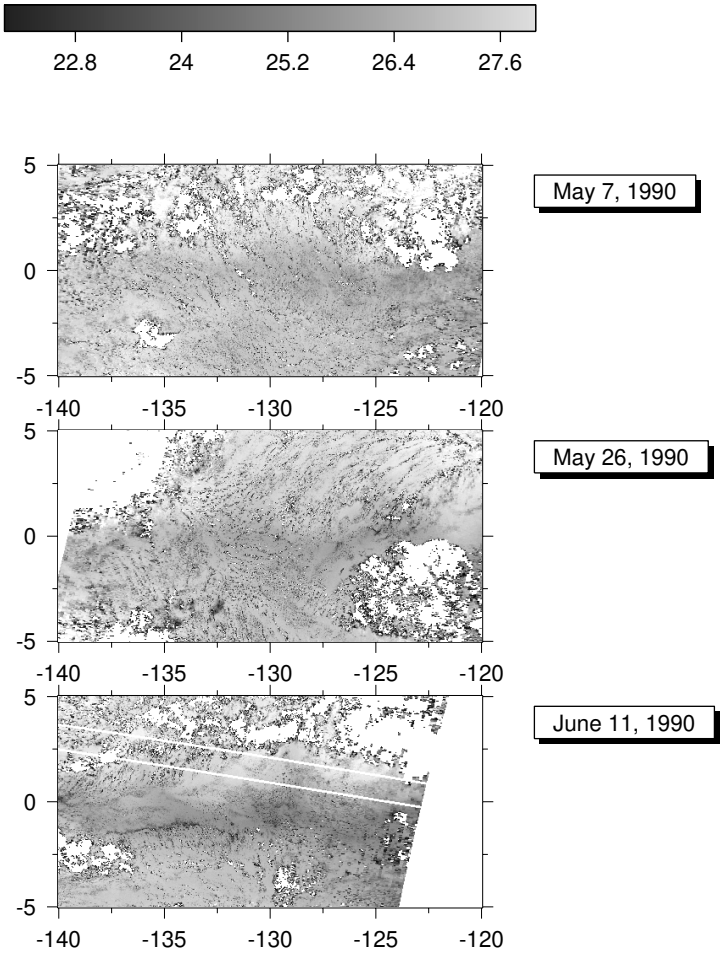

Figure 1.3: Series of satellite SST images of the Equatorial Pacific, showing increased upwelling strength during late Spring and early Summer, northern hemisphere. Dark shading represents cold water temperatures and light shading represents warmer temperatures. Upper frame was collected May 7, 1990, the middle frame was collected May 26, and the bottom June 11. The light band running horizontally across the figure is the equatorial upwelling region.

Chapter 2

Description of the Experiment

2.1 Field Programs

R/V Moana Wave cruise 90-10 (MW9010) in August, 1990, focused on the small-scale features of the North Equatorial Front itself. The sampling strategy during this cruise was driven by real-time analysis of satellite SST. Three closely spaced crossings were made on Aug 20 at 3.5°N by 129°W across a front in the western side of a perturbation (Figure 2.1). A 50 km counter-rotating box survey was conducted to coincide with a drifter launch at the northern tip of the perturbation at 4°N by 128°W. A single crossing of the front along the eastern side of the perturbation was conducted at 3°N by 127°W.

R/V Moana Wave cruise 90-12 (MW9012) in November, 1990, focused on the large scale dynamics of the equatorial instability. A 2° meridional by 3° zonal box survey (Figure 2.2) was conducted over the entire instability wave region, with a short excursion from the box pattern for a meridional sawtooth survey of the front in the region between two perturbations.

A series of cruises on the *R/V Thomas Thompson* were conducted in the TIWE region during the Joint Global Ocean Flux Study Equatorial Pacific (JGOFS EqPac) survey. This research was conducted to understand the biological implications of the North Equatorial Front [Yoder *et al.*, 1994]. Satellite data collected during this project will be discussed here, with a full treatment of the observations found in Johnson *et. al* [1996].

2.2 Instruments

During all field projects, Advanced Very High Resolution Radiometer (AVHRR) data from the NOAA polar orbiting satellites were collected from a shipboard receiving station. The Multi-Channel Sea Surface Temperature (MCSST) algorithm was used to produce maps of the SST over the TIWE study region; these data have a nominal resolution of 1.1 km, with highest resolution along the center of the satellite track, decreasing towards the edges. Gridded data were produced on a rectangular projection with a 1.25 km resolution. The North Equatorial Front was clearly seen in these data as a sharp boundary between the cold upwelling water and the surrounding water, nearly 2°C warmer.

During MW9010, Lagrangian drifters were deployed in the vicinity of the front in a spiral pattern to investigate the small-scale velocity field and to make estimates of frontal convergence rates. During MW9012, drifters were deployed at regular intervals throughout the cruise to investigate the large-scale velocity field.

World Ocean Circulation Experiment (WOCE) style "holey-sock" drifters were used in this project because of their tested ability to accurately follow the horizontal motions of water parcels [Niiler *et al.*, 1987; Niiler *et al.*, 1995]. Based on a mean wind velocity of 8 ms^{-1}, a velocity error of less than 0.01 ms^{-1} is expected using this drifter design. All drifters used were drogued at a mean depth of 15 m. Tracking during the cruise was provided directly by the on-board satellite receiver. A drifter mounted on the ship was used as a reference platform for these positions. Quality controlled data provided by Service ARGOS with a stated resolution of 300 m was used for post-processing and scientific analysis.

A 150 kHz shipboard-mounted Acoustic Doppler Current Profiler (ADCP) using a Global Positioning System (GPS) for navigation yielded velocity profiles to 300 m with an 8 m vertical resolution. Profiles were vector averaged in 5 minute ensembles, referenced against average ship velocity. A reference layer mean was removed from each profile before averaging and added back to the ensemble average. This prevented variations in ship's velocity from contaminating the estimated oceanic shear. Details on ADCP processing can be found in Firing *et al.* [1994].

A Conductivity, Temperature, and Depth (CTD) profiler was used during MW9010 and MW9012 to collect hydrographic data in the study area. Hydrographic casts were conducted to a depth of 300m, using dual temperature and conductivity sensors. Data were collected at 12 Hz during MW9010 and 24 Hz during MW9012, giving 12 and 24 samples per meter at the nominal lowering and raising rates of 1 ms^{-1}. Rates were reduced to 0.5 ms^{-1} in the vicinity of sharp gradients in any water property, such as the permanent 150 m thermocline. Niskin bottle samples were collected on alternate casts to ensure calibration accuracy. When bottle samples were collected one with the bottle as close to the surface as possible and one at 300 dbar pressure. Details on the CTD processing can be found in Trefois *et al.* [1993].

During MW9010, hydrographic stations were made along the frontal crossing on the eastern side of the perturbation, as well as on the return transect every $50 \sim 100$ km to 10°N. During MW9012, hydrographic stations were made at 25 km intervals along the ship track during the box survey.

In addition to conventional hydrography, a towed, undulating platform, the SeaSoar, was used to obtain continuous profiles of hydrographic data as the ship was underway. The SeaSoar was fitted with a conventional CTD profiler and yielded profiles from a

depth of 10 m to 300 m every 15 minutes at a ship velocity of 8 knots. Details on the SeaSoar deployment and processing are found in Appendix A.

During MW9010, the SeaSoar was deployed during the frontal crossing on the western side of the perturbation and during the box survey at the northern tip of the perturbation. During MW9012, the SeaSoar was used during some legs of the large box survey and during the sawtooth survey. Use of the SeaSoar was prevented by mechanical problems with the platform after day 330.